JOC*Article*

Zigzag Molecules from Pyrene-Modified Carbazole Oligomers: Synthesis, Characterization, and Application in OLEDs

Zujin Zhao,[†] Xinjun Xu,[‡] Hongbo Wang,[†] Ping Lu,*[,†] Gui Yu,[‡] and Yunqi Liu*[,‡]

Department of Chemistry, Zhejiang University, Hangzhou 310027, People's Republic of China, and Laboratory of Organic Solids, Institute of Chemistry, Chinese Academy of Sciences, Beijing 100080, People's Republic of China

pinglu@zju.edu.cn

Received September 21, 2007

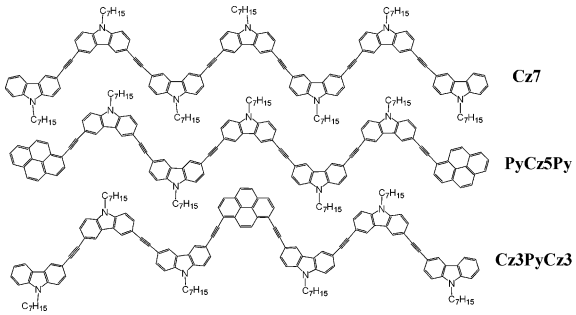

A series of monodisperse, pyrene-modified oligocarbazoles were synthesized and fully characterized. Carbazoles were linked by ethynylene through the 3- and 6-positions, forming a zigzag molecular backbone and stable, size-independent absorption, and emission were observed from these oligomers in solutions because their conjugation length was confined. Oligomers with pyrene exhibited much higher fluorescence quantum yields than those of oligomers without it. Different positions of pyrene in the oligocarbazole main chain resulted in a remarkable change in absorption and emission spectra. Moreover, devices with four different architectures (types 1−4) based on these oligomers were fabricated and investigated. Pyrene-modified carbazole oligomers exhibited bifunctional properties (light-emitting and hole-transport). Moreover, these devices showed moderate performances; for example,the device based on **Cz3PyCz3** presented an external quantum efficiency of 0.69% and a maximum brightness of 1782 cd/m^2 at 13.5 V, which indicated these oligomers were promising optoelectric materials.

1. Introduction

Conjugated oligomers are subjected to important investigations from both academic and industrial laboratories[1] due to their promising applications, such as organic light-emitting diodes (OLEDs),[2] solar cells,[3] field-effect transistors (FETs),[4] and models[5] to understand the fundamental properties of their analogous polydisperse polymers. Significant developments in modern synthetic chemistry, especially the chemistry of carbon−carbon bond formation (through Kumada, Stille, Yamamoto, Suzuki, Heck, and Sonogashira couplings, etc.),[6] have allowed the precise control on the orientation of functional groups in oligomers and thus the resulting optimized physical properties. Depending on these advanced synthetic techniques, different conjugated building blocks (thiophene, pyrrole, phenylene, and fluorene moieties, etc.) have been developed and utilized.

Carbazole and its derivatives have been widely used as a functional building block in the fabrication of the organic photoconductors, nonlinear optical materials, and photorefractive

* Corresponding author. Tel: + 86-571-879- 52543.
[†] Zhejiang University.
[‡] Chinese Academy of Sciences.

(1) Skotheim, T. A., L. Elsenbaumer, R., Reynolds, J. R., Eds. *Handbook of Conducting Polymers*, 2nd ed.; Marcel Dekker: New York, 1998.
(2) (a) van Hutten, P. F.; Wildeman, J.; Meetsma, A.; Hadziioannou, G. *J. Am. Chem. Soc.* **1999**, *121*, 5910. (b) Goodson, T., III; Li, W.; Gharavi, A.; Yu, L. *Adv. Mater.* **1997**, *9*, 639.
(3) (a) Noma, N.; Tsuzuki, T.; Shirota, Y. *Adv. Mater.* **1995**, *7*, 647. (b) Eckert, J.-F.; Nicoud, J.-F.; Nierengarten, J.-F.; Liu, S.-G.; Echegoyen, L.; Barigelletti, F.; Armaroli, N.; Ouali, L.; Krasnikov, V.; Hadziioannou, G. *J. Am. Chem. Soc.* **2000**, *122*, 7467.
(4) Schon, J. H.; Dodabalapur, A.; Kloc, C.; Batlogg, B. *Science* **2000**, *290*, 963.
(5) Martin, R. E.; Diederich, F. *Angew. Chem., Int. Ed.* **1999**, *38*, 1350.
(6) Morin, J.-F.; Drolet, N.; Tao, Y.; Leclerc, M. *Chem. Mater.* **2004**, *16*, 4619.

10.1021/jo702075r CCC: $40.75
Published on Web 12/21/2007

materials[7] due to their specific optical and electrochemical properties. In the field of OLED technology, carbazole derivatives are usually used as promising blue light-emitting materials.[8] Interestingly, white light is also achieved from carbazole dimers or oligomers serving as a single-emitting-component layer in device.[9] Meanwhile, a great many of carbazole homopolymers or oligomers as well as carbazole-containing polymers or small molecules, such as widely used PVK (polyvinylcarbazole) and CBP (*N*,*N*′-dicarbazolyl-4, 4′-biphenyl), are of excellent hole-transport ability, due to the electron-donating capabilities.[10] Furthermore, carbazole derivatives are of high triplet energy and capable of using host materials in highly efficient blue, green, or red electrophosphorescence devices[11] due to efficient energy transfer from these hosts to doped triplet emitters. Recently, many reports have discussed their applications in light-emitting dendrimers with carbazole-based dendrons incorporated at antennal positions for efficient energy harvest and transfer.[12] In particular, carbazole-based dendrons can also be used to construct phosphorescent dendrimers,[13] in which high triplet energy of carbazole is transferred to the core affording an excellent efficiency of device and avoiding phase separation in some doped systems. On the other hand, chemically, the carbazole moiety can be easily modified at its 3-, 6-, or 9-positions and covalently linked to other molecular moieties,[14] while its 2- and 7-positions are comparably stable. Nevertheless, there are also reports on carbazole oligomers linked together through their 2- and 7-positions.[6,15] These compounds can be used as models to investigate structure−property relationship of corresponding polymers or adopted as optoelectronic materials. Besides these remarkable advantages, it is also recognized that the thermal stability or glass-state durability of organic compounds can be greatly improved by introducing carbazoles into the core structures.[16] Thus, structural modification of carbazole for improved optoelectronic performance of materials, such as hole-transport/emitting/electron-transport (three-in-one) for simplified OLED architecture, is feasible, challengeable, and valuable.[17]

Here, we wish to report the synthesis and characterization of a series of well-defined, monodisperse, ethynylene-linked oligocarbazoles. Two considerations were taken into our mind using the oligocarbazole as the main chain. First, from a synthetic point of view, well-defined and highly pure chromophores could be obtained, which would offer improved stability and comparable optical and electronic properties and facilitate systematic investigation of structure−property relationship. Second, oligocarbazoles linked through the 3,6-positions had defined efficient conjugation length and thus could prevent undesirable optical defects arising from dispersed molecular size. Moreover, comparing with single or double bond linked carbazole oligomers or polymers, triple bond linked ones are not abundantly reported. On the other hand, pyrene was selected and introduced to oligocarbazole because it is rigid and highly fluorescent and its derivatives have been wildly used as optoelectronic materials.[18] After investigation of these oligomers in different types of devices, our preliminary results indicated that these pyrene-functionalized, ethynylene-linked oligocarbazoles could be used as both light-emitting and hole-transporting materials in efficient OLEDs.

2. Results and Discussion

2.1. Synthesis. A Pd/Cu-catalyzed Sonogashira coupling reaction was used to build ethynylene-linked molecules. Detailed experimental conditions for oligomer formation were similar to the published method.[19] 1-Ethynylpyrene and 1,8-diethynylpyrene were prepared according to the reference.[20] The synthetic approach to necessary intermediates **1**−**14** is outlined in Scheme 1. Alkylation of 3-iodo-9*H*-carbazole afforded 9-heptyl-3-iodo-9*H*-carbazole (**1**) in 94% yield. Pd/Cu-catalyzed coupling of **1** and 3-methyl-1-butyn-3-ol provided **2**, and subsequent treatment of **2** with base generated **3** in 79% total yield. Similar procedures were performed from 3,6-diiodo-9*H*-carbazole to obtain 9-heptyl-3,6-diiodo-9*H*-carbazole (**4**) and 3,6-diethynyl-9-heptyl-9*H*-carbazole (**6**) in 91% and 54% yields, respectively. Treatment of **3** with 3 equiv of **4** in the presence of CuI/Pd(PPh$_3$)$_2$Cl$_2$/Ph$_3$P/NEt$_3$ afforded intermediate (**7**) in 72%

(7) (a) Zhang, Y.; Wada, T.; Sasabe, H. *J. Mater. Chem.* **1998**, *8*, 809. (b) Zhang, Y.; Wada, T.; Wang, L.; Sasabe, H. *Chem. Mater.* **1997**, *9*, 2798. (c) Zhang, Y.; Wada, T.; Wang, L.; Sasabe, H. *Macromol. Chem. Phys.* **1996**, *197*, 1877. (d) Sonntag, M.; Kreger, K.; Hanft, D.; Strohriegl, P. *Chem. Mater.* **2005**, *17*, 3031.

(8) (a) Adhikari, R. M.; Mondal, R.; Shah, B. K.; Neckers, D. C. *J. Org. Chem.* **2007**, *72*, 4727. (b) Zhao, Z.; Zhang, P.; Wang, F.; Wang, Z.; Lu, P.; Tian, W. *Chem. Phys. Lett.* **2006**, *423*, 293. (c) Xing, Y.; Xu, X.; Zhang, P.; Tian, W.; Yu, G.; Lu, P.; Liu, Y.; Dao, D. *Chem. Phys. Lett.* **2005**, *408*, 169. (d) Cha, S. W.; Jin, J.-I. *J. Mater. Chem.* **2003**, *13*, 479. (e) Shen, J.-Y.; Yang, X.-L.; Huang, T.-H.; Lin, J. T.; Ke, T.-H.; Chen, L.-Y.; Wu, C.-C.; Yeh, M.-C. P. *Adv. Funct. Mater.* **2007**, *17*, 983. (f) Justin Thomas, K. R.; Velusamy, M.; Lin, J. T.; Tao, Y.-T.; Chuen, C.-H. *Adv. Funct. Mater.* **2004**, *13*, 387.

(9) (a) Liu, Y.; Nishiura, M.; Wang, Y.; Hou, Z. *J. Am. Chem. Soc.* **2006**, *128*, 5592. (b) Li, J. Y.; Liu, D.; Ma, C. W.; Lengyel, O.; Lee, C.-S.; Tung, C.-H.; Lee, S. T. *Adv. Mater.* **2004**, *16*, 1583. (c) Zhao, Z.; Zhao, Y.; Lu, P.; Tian, W. *J. Phys. Chem. C* **2007**, *111*, 6883.

(10) (a) Liu, B.; Yu, W.; Lai, Y.; Huang, W. *Chem. Mater.* **2001**, *13*, 1984. (b) Xia, C.; Advincula, R. C. *Macromolecules* **2001**, *34*, 5854. (c) Stephan, O.; Vial, J.-C. *Synth. Met.* **1999**, *106*, 115. (d) Promarak, V.; Ichikawa, M.; Sudyoadsuk, T.; Saengsuwan, S.; Jungsuttiwong, S.; Keawin, T. *Synth. Met.* **2007**, *157*, 17. (e) Li, J.; Ma, C.; Tang, J.; Lee, C.-S.; Lee, S. T. *Chem. Mater.* **2005**, *17*, 615. (f) Qian Zhang, Q.; Chen, J.; Cheng, Y.; Wang, L.; Ma, D.; Jing, X.; Wang, F. *J. Mater. Chem.* **2004**, *14*, 895.

(11) (a) Chen, Y.-C.; Huang, G.-S.; Hsiao, C.-C.; Chen, S.-A. *J. Am. Chem. Soc.* **2006**, *128*, 5592. (b) Tsai, M.-H.; Hong, Y.-H.; Chang, C.-H.; Su, H.-C.; Wu, C.-C.; Matoliukstyte, A.; Simokaitiene, J.; Grigalevicius, S.; Grazulevicius, J. V.; Hsu, C.-P. *Adv. Mater.* **2007**, *19*, 862. (c) Brunner, K.; Dijken, A.; Börner, H.; Bastiaansen, J. J. A. M.; Kiggen, K. M. M.; Langeveld, B. M. W. *J. Am. Chem. Soc.* **2004**, *126*, 6035. (d) Shih, P.-I.; Chiang, C.-L.; Dixit, A. K.; Chen, C.-K.; Yuan, M.-C.; Lee, R.-Y.; Chen, C.-T.; Diau, E. W.-G.; Shu, C.-F. *Org. Lett.* **2006**, *8*, 2799.

(12) (a) Loiseau, F.; Campagna, S.; Hameurlaine, A.; Dehaen, W. *J. Am. Chem. Soc.* **2005**, *127*, 11352. (b) Wong, K.-T.; Lin, Y.-H.; Wu, H.-H.; Fungo, F. *Org. Lett.* **2007**, *9*, 4531. (c) Xu, T.; Lu, R.; Liu, X.; Zheng, X.; Qiu, X.; Zhao, Y. *Org. Lett.* **2007**, *9*, 797.

(13) (a) Ding, J.; Gao, J.; Cheng, Y.; Xie, Z.; Wang, L.; Ma, D.; Jing, X.; Wang, F. *Adv. Funct. Mater.* **2006**, *16*, 575. (b) Kwon, T.-H.; Kim, M. K.; Kwon, J.; Shin, D.-Y.; Park, S. J.; Lee, C.-L.; Kim, J.-J.; Hong, J.-I. *Chem. Mater.* **2007**, *19*, 3673.

(14) Joule, J. A. *Adv. Heterocycl. Chem.* **1984**, *35*, 83.

(15) Strohriegl, P.; Sonntag, M. *Chem. Mater.* **2004**, *16*, 4736.

(16) (a) Tao, X. T.; Miyata, S.; Sasabe, H.; Zhang, G. J.; Wada, T.; Jiang, M. H. *Appl. Phys. Lett.* **2001**, *78*, 279. (b) Lamansky, S.; Djurovich, P.; Murphy, D.; Feras, A.-R.; Lee, H.-E.; Adachi, C.; Burrows, P. E.; Forrest, S. R.; Thompson, M. E. *J. Am. Chem. Soc.* **2001**, *123*, 4304.

(17) (a) Kundu, P.; Thomas, K. R. J.; Lin, J. T.; Tao, Y.-T.; Chien, C.-H. *Adv. Funct. Mater.* **2003**, *13*, 445. (b) Thomas, K. R. J.; Lin, J. T.; Tao, Y.-T.; Ko, C.-W. *J. Am. Chem. Soc.* **2001**, *123*, 9404. (c) Thomas, K. R. J.; Lin, J. T.; Tao, Y.-T.; Ko, C.-W. *Adv. Mater.* **2000**, *12*, 1949. (d) Thomas, K. R. J.; Velusamy, M.; Lin, J. T.; Tao, Y.-T.; Chuen, C.-H. *Adv. Funct. Mater.* **2004**, *14*, 387.

(18) (a) Tao, S.; Peng, Z.; Zhang, X.; Wang, P.; Lee, C.-S.; Lee, S.-T. *Adv. Funct. Mater.* **2005**, *15*, 1716. (b) Tang, C.; Liu, F.; Xia, Y.-J.; Wei, A.; Li, S.-B.; Fan, S.-B.; Fan, Q.-L.; Huang, W. *J. Mater. Chem.* **2006**, *16*, 4074. (c) Moggia, F.; Videlot-Ackermann, C.; Ackermann, J.; Raynal, P.; Brisset, H.; Fages, F. *J. Mater. Chem.* **2006**, *16*, 2380. (d) Lo, M. Y.; Zhen, C.; Lauters, M.; Jabbour, G. E.; Sellinger, A. *J. Am. Chem. Soc.* **2007**, *129*, 5808.

(19) Lee, S. H.; Nakamura, T.; Tsutsui, T. *Org. Lett.* **2001**, *3*, 2005.

(20) Leroy-Lhez, S.; Fages, F. *Eur. J. Org. Chem.* **2005**, *13*, 2684.

SCHEME 1[a]

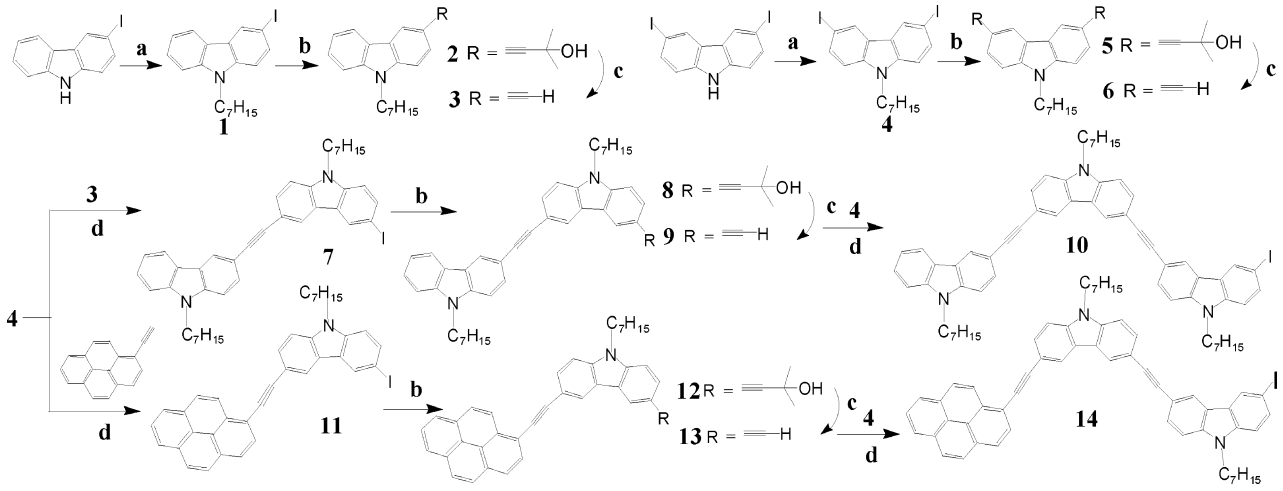

[a] Key: (a) *n*-$C_7H_{15}Br$, KOH, tetrabutylammonium hydrogen sulfate, acetone, rt; (b) 3-methyl-1-butyn-3-ol, CuI, $Pd(PPh_3)_2Cl_2$, Ph_3P, NEt_3, N_2, reflux; (c) KOH, 2-propanol, reflux.

SCHEME 2[a]

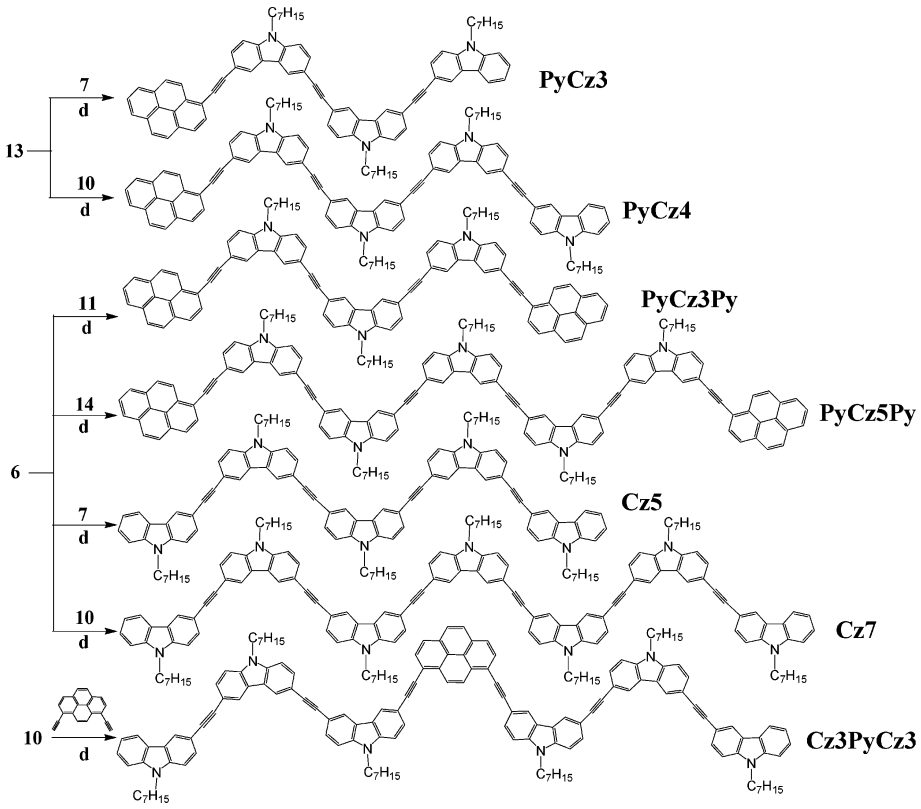

[a] Key: (d) CuI, $Pd(PPh_3)_2Cl_2$, Ph_3P, NEt_3, N_2, reflux.

yield after separation by column chromatography. Compound **7** was then converted to **9** in 75% yield after cross-coupling and subsequent deprotection. Similarly, **13** was obtained from **11** in 63% yield. Compounds **10**, **11**, and **14** were synthesized in 67%, 70%, and 62% yields, respectively.

Final construction to target molecules is illustrated in Scheme 2. **PyCz3** and **PyCz4** were obtained in 55% and 46% yields, respectively. Coupling **6** with 2 equiv of **11** led to the pyrene-anchored **PyCz3Py** in 58% yield. **PyCz5Py**, **Cz5**, and **Cz7** were synthesized by similar procedures in 45%, 61%, and 51% yields, respectively. Treatment of 1,8-diethynylpyrene with 2 equiv of **10** afforded **Cz3PyCz3** in 39% yield. The structures of the final oligomers were verified by ^1H and ^{13}C NMR spectroscopy, MALDI-TOF MS measurement, and element analysis. Moreover, due to the presence of the flexible *n*-heptyl substituents, all of these synthesized compounds were soluble in common organic solvents, such as CH_2Cl_2 and THF.

2.2. Optical Properties. The UV−vis absorption and PL properties of these synthesized oligomers in dilute solutions and in the solid state are presented in Table 1. Absorption spectra of these compounds were complex with multiple overlapping broad bands. Some representative spectra are shown in Figure

TABLE 1. Optical, Thermal, and Electrochemical Properties of Oligomers

	abs[a] (nm)		em (nm)								
compd	THF	film	cyclohexane	THF	film	Φ^b	$E_g{}^c$ (eV)	$E^{\circ x}{}_{onset}{}^d$ (V)	$E^{\circ x}{}_p{}^d$ (V)	HOMO/LUMO[e](eV)	$T_g/T_mT_d{}^f$ (°C)
PyCz3	405	415	411 (436)	446	467	0.92	2.89	0.89	1.12, 1.84	−5.29/−2.40	94/NA/446
PyCz4	405	415	411 (436)	446	468	0.89	2.89	0.80	1.02, 1.76	−5.28/−2.39	104/NA/458
PyCz3Py	405	417	411 (436)	446	469	0.88	2.86	0.95	1.04, 1.76	−5.35/−2.49	101/190/466
PyCz5Py	405	417	450	449	472	0.82	2.85	0.86	0.97, 1.72	−5.27/−2.42	125/NA/476
Cz3PyCz3	443	462	460 (487)	469	513	0.83	2.64	0.94	1.17, 1.99	−5.34/−2.70	165/NA/468
Cz5	363	367	401	(384) 405	456	0.38	3.19	0.77	1.00, 1.77	−5.17/−1.98	119/180/449
Cz7	364	369	400	(381) 405	467	0.32	3.18	0.78	0.96, 1.69	−5.18/−2.00	138/209/454

[a] First absorption peak. [b] Measured in THF solutions using DPA as a standard. [c] Determined from UV−vis absorption spectra [d] $E^{\circ x}{}_{onset}$ = onset oxidation potential; $E^{\circ x}{}_p$ = oxidation peak potential; potentials vs Ag/AgCl, working electrode Pt, 0.1 M $Bu_4NPF_6-CH_2Cl_2$, scan rate 100 mV/s. [e] HOMO = $E^{\circ x}{}_{onset}$ + 4.4 eV; LUMO = HOMO − E_g eV. [f] Measured by DSC and TGA analysis in N_2 at a heating rate of 10 °C/min; NA, not observed.

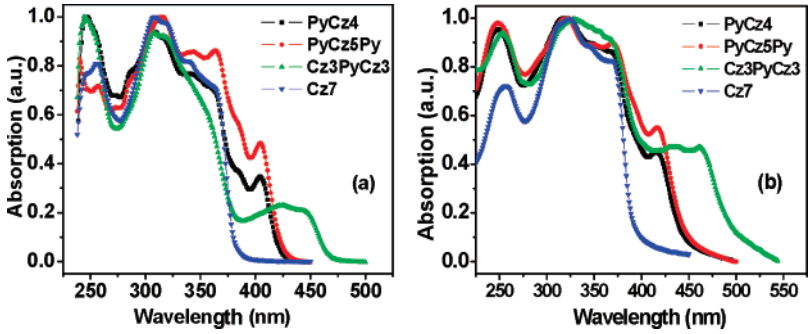

FIGURE 1. UV−vis absorption spectra of some compounds in THF (a) and in thin neat film (b).

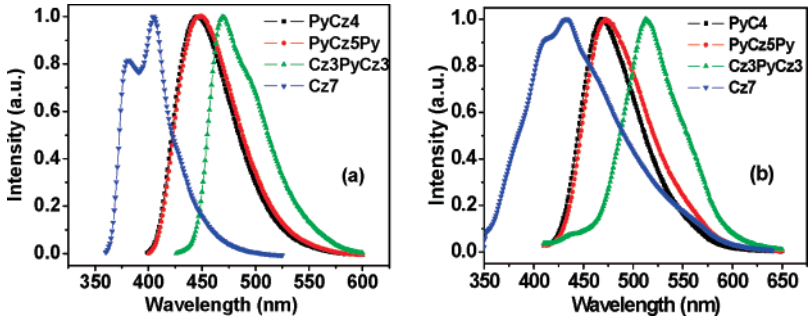

FIGURE 2. PL emission spectra of some compounds in THF (a) and in thin neat films (b).

1. **Cz5** and **Cz7** exhibited the same maximum absorption peaks at about 363 nm in THF solutions. Pyrene-end-capped oligomers **PyCz3**, **PyCz4**, **PyCz3Py**, and **PyCz5Py** exhibited the same maximum absorption peaks at 405 nm due to their same efficient conjugation length, while pyrene-centered oligomer **Cz3PyCz3** exhibited a maximum absorption peak at 443 nm, which was red-shifted by 38 nm with respect to those of oligomers with pyrene at their ends. The $\pi-\pi^*$ energy gaps (E_g, Table 1) of these oligomers were calculated from the UV−vis absorption threshold. It was obvious that the E_g's of oligomers could be greatly reduced by introduction of pyrene at the center of oligomer backbone. In the case of solid states, absorption spectra of these oligomers were slightly red-shifted compared to those in solutions, which was ascribed to the enhanced intermolecular interaction.

Figure 2 displays the PL emission spectra of these oligomers excited at 350 nm. These oligomers showed a blue to green PL emission with the maximum emission peaks varying from 405 to 469 nm in THF solutions. Large Stokes' shifts, about 40 nm in THF, were observed for these oligomers, except **Cz3PyCz3**, indicating that the ground-state conformations (more twisted) of these oligomers were different from those in excited states

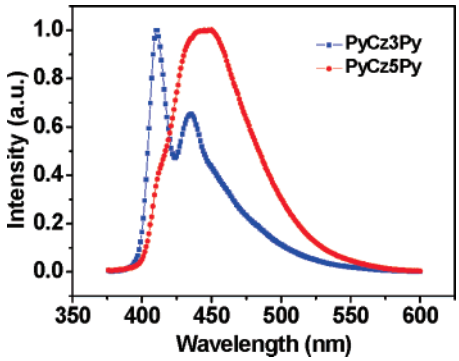

FIGURE 3. PL emission spectra of **PyCz3Py** and **PyCz5Py** in cyclohexane.

(more coplanar structure).[6] Moreover, PL emission spectra of **PyCz3**, **PyCz4**, and **PyCz3Py** were solvent dependent. With the increment of the solvent polarity (from cyclohexane to THF), large red shifts (35 nm) were observed (Table 1). It suggested that the excited states of these pyrene-modified oligocarbazoles possessed more polar character, and polar environments efficiently enhanced the intramolecular charge transfer from

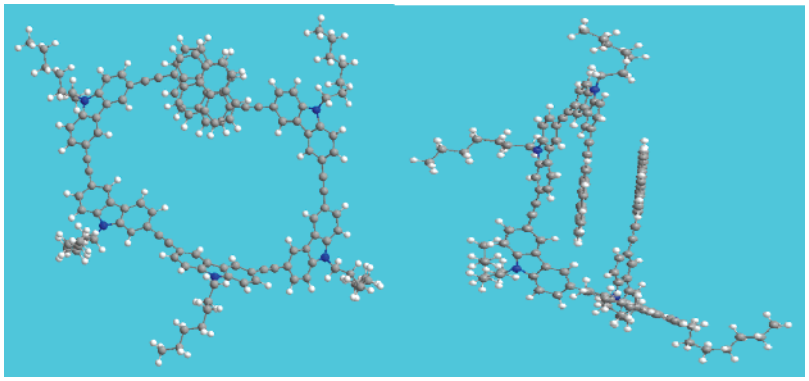

FIGURE 4. Molecule modeling of **PyCz5Py** in cyclohexane solution: front view (left) and side view (right).

carbazole donor to pyrene acceptor. Interestingly, **PyCz5Py** exhibited a broad, featureless, and red-shifted emission (450 nm) in cyclohexane solution (Figure 3) with respect to that of **PyCz3Py**, although both oligomers had an identical efficient conjugation length.[21] In fact, this red-shifted emission was quite similar to the excimer emission of pyrene (about 450 nm).[22] With regard to the self-assembling of macrocycles composed of ethynylene-linked carbazoles[23] in poor solvent such as cyclohexane, we inferred that this red shift arose from the intramolecular $\pi-\pi$ stacking of two pyrenes at both ends of **PyCz5Py**. The main chain length of **PyCz5Py** was theoretically and practically suitable for two pyrenes to be parallel and close enough to form the excimer. Figure 4 displays the molecular modeling of **PyCz5Py** in cyclohexane solution. However, in THF solution, emission of **PyCz5Py** resembled to those emission characteristics of **PyCz3**, **PyCz4**, and **PyCz3Py** with intramolecular charge-transfer character. Concerning PL emissions of all oligomers in the solid state, the shapes of emission spectra were similar to those in THF solutions, respectively, but with bathochromical shifts in the maximum emission wavelengths. As seen from Table 1, it seemed that incorporation of pyrene could reduce this bathochromical shift to some extent. For example, emission of **Cz5** in the solid state red-shifted by 51 nm in comparison with that in THF solution, while emission of **PyCz4** in the solid state showed only 22 nm red shift.

In general, the carbazole oligomers or polymers were of low fluorescence quantum yields and were not suitable as OLED emitters. By introduction of pyrene, quantum yields of oligomers were significantly increased. For instance, quantum yields of **Cz5** and **Cz7** were 0.38 and 0.32 in THF solutions, respectively, while pyrene-modified oligomers exhibited much higher quantum yields measured between 0.82 and 0.92. The reason might be that excitons could be well confined in the low-band gap, highly chromophoric segment (pyrene). In the case of oligomers without pyrene, some energy loss might happen during the process of exciton migration.[24] Moreover, slightly decrement of quantum yields with the increment of the molecular size was observed (**PyCz3** vs **PyCz4**, **PyCz3Py** vs **PyCz5Py**), which might be due to the faster nonradiative energy decay in the larger molecules.

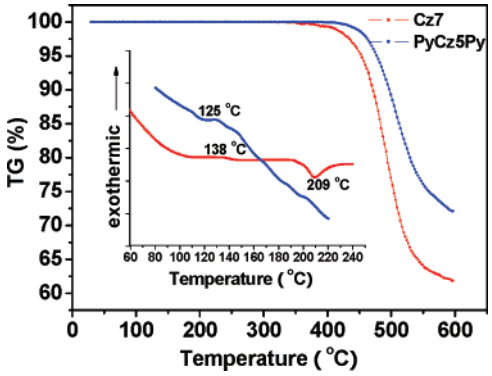

FIGURE 5. TGA and DCS (inset) thermograms of **Cz7** and **PyCz5Py** in N_2 at a heating rate of 10 °C/min.

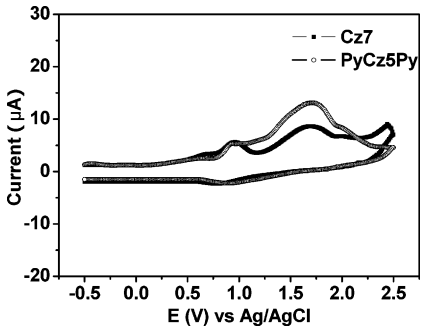

FIGURE 6. Cyclic voltammograms of **Cz7** and **PyCz5Py** (0.5 mM) in 0.1 M $Bu_4NPF_6-CH_2Cl_2$, scan rate 100 mV/s.

2.3. Thermal Stabilities. Thermal stabilities of these oligomers were examined by differential scanning calorimetry (DSC) and thermogravimetric analysis (TGA) in N_2 at a heating rate of 10 °C/min, and the results are listed in Table 1. Figure 5 shows the TGA and DSC thermgrams of **Cz7** and **PyCz5Py** as an example. All of these oligomers exhibited high glass-transition temperatures (T_g's) in the range of 94−165 °C. The T_g's of some oligomers appear to be relatively higher than those of widely used hole-transport materials, such as 1,4-bis(1-naphthylphenylamino)diphenyl (α-NPD, T_g = 100 °C), 4,4′-bis(4-(*N*-(1-naphthyl)-*N*-phenylamino)phenyl)biphenyl (NPB, T_g = 96 °C), and 1,4-bis(phenyl-*m*-tolylamino)diphenyl (TPD, T_g

(21) (a) Zhao, Z.; Xu, X.; Wang, F.; Yu, G.; Lu, P.; Liu, Y.; Zhu, D. *Synth. Met.* **2006**, *156*, 209. (b) Wang, Z.; Shao, H.; Ye, J.; Tang, L.; Lu, P. *J. Phys. Chem. B* **2005**, *109*, 19627.

(22) Nandy, R.; Subramoni, M.; Varghese, B.; Sankararaman, S. *J. Org. Chem.* **2007**, *72*, 938.

(23) (a) Zhang, W.; Moore, J. S. *J. Am. Chem. Soc.* **2004**, *126*, 12796. (b) Balakrishnan, K.; Datar, A.; Zhang, W.; Yang, X.; Naddo, T.; Huang, J.; Zuo, J.; Yen, M.; Moore, J. S.; Zang, L. *J. Am. Chem. Soc.* **2006**, *128*, 6576. (c) Zhao, T.; Liu, Z.; Song, Y.; Xu, W.; Zhang, D.; Zhu, D. *J. Org. Chem.* **2006**, *71*, 7422.

(24) Li, Y.; Ding, J.; Day, M.; Tao, Y.; Lu, J.; D'iorio, M. *Chem. Mater.* **2004**, *16*, 2165.

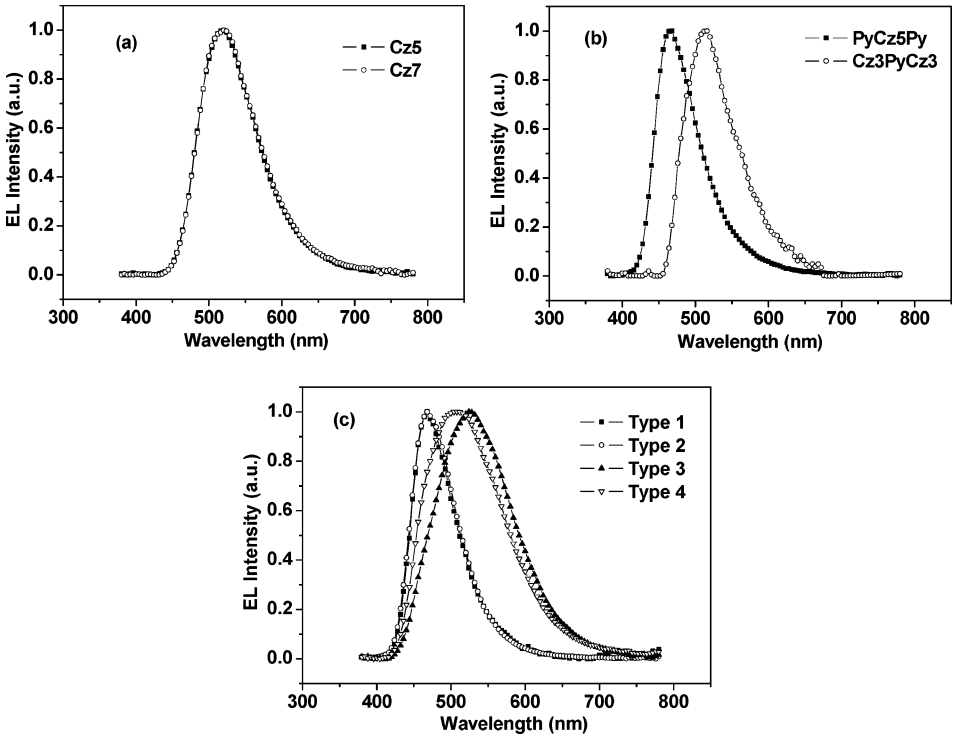

FIGURE 7. EL spectra: (a) type 3 devices based on **Cz5** and **Cz7**; (b) type 2 devices based on **PyCz5Py** and **Cz3PyCz3**; (c) type 1−4 devices based on **PyCz4**.

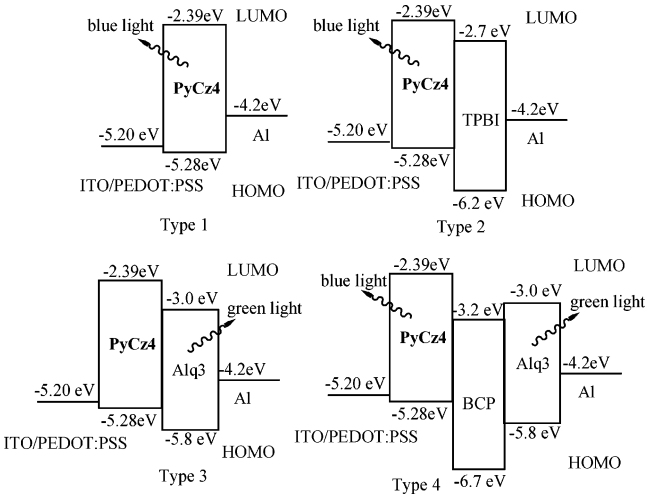

FIGURE 8. Energy alignments in type 1−4 devices based on **PyCz4**.

= 60 °C).[17c,25] Moreover, **Cz3PyCz3** exhibited much higher T_g (165 °C) than those of others. The T_g enhancement of **Cz3PyCz3** might be due to its center position of pyrene at oligomer backbone. Melting points of **PyCz3Py** (190 °C), **Cz5** (180 °C), and **Cz7** (209 °C) were detected, while those of others were not observed. The thermal stabilities of compounds were further determined by TGA measurement. High decomposition temperatures (T_d's, corresponding to a 5% weight loss), in the range of 446−476 °C, were observed from these oligomers. All of these results indicated that these synthesized oligomers were of high morphological and thermal stabilities, which was a critical issue for device stability and lifetime.

2.4. Cyclic Voltammetric Studies. The electronic properties of these compounds were investigated by cyclic voltammetry at room temperature and the results are listed in the Table 1. Figure 6 shows cyclic voltammograms (CVs) of **Cz7** and **PyCz5Py** as an example. All of these oligomers displayed two irreversible oxidation peaks (first peak, 0.96−1.17 V; second peak, 1.72−1.99 V), which might be due to the formation of cation and dication radical, respectively. The highest occupied molecular orbital (HOMO) and lowest unoccupied molecular orbital (LUMO) energy levels of **Cz5** (−5.17, −1.98 eV) and **Cz7** (−5.18, −2.00 eV) were very close to those of tercarbazole (−5.2, −1.6 eV)[15] or the related homopolymer (−5.1, −2.0 eV).[26] It suggested that HOMO levels of **Cz5** and **Cz7** were close to the HOMO level of PEDOT:PSS (−5.2 eV), indicating a good hole injection contact. Moreover, their LUMO levels represented a small barrier for electron injection from a commonly used cathode such as barium, which has a work function of −2.2 eV.[26] Adjusting the structure by inserting pyrene into the main chain improved the electronic communication between carbazole and pyrene. Thus, HOMO and LUMO energy levels of pyrene-modified compounds were apparently raised compared to those of **Cz5** and **Cz7**. Furthermore, the HOMO and LUMO energy levels of these oligomers were comparable to those of widely used hole transporting materials (NPB: HOMO, −5.2 eV; LUMO, −2.2 eV),[25] and therefore, these compounds might be used for hole-transporting materials in OLEDs.

2.5. Electroluminescent Properties. First, hole-transport abilities of oligomers (**Cz5** and **Cz7**) were investigated in OLEDs with a configuration of type 3 (ITO/PEDOT:PSS (30 nm)/**Cz5** or **Cz7**(50 nm)/Alq_3(45 nm)/Al(100 nm)), in which

(25) Li, J.; Liu, D.; Lee, C.-S.; Kwong, H.-L.; Lee, S. *Chem. Mater.* **2005**, *17*, 1208.

(26) Dijken, A.; Bastiaansen, J. J. A. M.; Kiggen, N. M. M.; Langeveld, B. M. W.; Rothe, C.; Monkman, A.; Bach, I.; Stössel, P.; Brunner, K. *J. Am. Chem. Soc.* **2004**, *126*, 7718.

TABLE 2. Summary of Device[a] Performances

compd	device	EL (nm)	fwhm (nm)	onset voltage (V)	$h_{max,ext}$(%)	$h_{max,L}$(cd/A)	L_{max}(cd/m^2, V)
Cz5	type 3	520	92	5.6	0.70	1.89	2138, 13
Cz7	type 3	520	93	8.4	0.23	0.63	326, 16.5
Cz3PyCz3	type 2	516	86	4.6	0.69	1.87	1782, 13.5
PyCz5Py	type 2	468	68	4.7	0.39	0.56	667, 11
PyCz4	type 1	468	66	NA	NA	NA	0.49, 4.6
	type 2	468	70	4.1	0.59	0.87	987, 10
	type 3	524	123	3.4	0.40	1.08	1891, 8.5
	type 4	504	126	3.7	0.65	1.64	1628, 13

[a] Devices: type 1, ITO/PEDOT/PSS (30 nm):oligomer (50 nm)/Al (100 nm); type 2, ITO/PEDOT:PSS (30 nm)/oligomer (50 nm)/TPBI (20 nm)/Al (100 nm); type 3, ITO/PEDOT:PSS (30 nm)/oligomer (50 nm)/Alq_3 (45 nm)/Al (100 nm); type 4, ITO/PEDOT:PSS (30 nm)/oligomer (50 nm)/BCP (15 nm)/Alq_3 (45 nm)/Al (100 nm). *J-V-L* characteristics and efficiency spectra of OLEDs are given in the Supporting Information.

PEDOT:PSS was used as a hole-injection layer and Alq_3 was used as an emitting layer as well as electron-transporting and hole-blocking layer. Both devices showed identical EL peaks at 520 nm (Figure 7a), originated from Alq_3, indicating that both **Cz5** and **Cz7** served as hole-transporting materials only and did not function as emitter. The device based on **Cz5** exhibited a maximum brightness of 2138 cd/m^2 at 13 V and a maximum external quantum efficiency of 0.70% as well as an onset voltage of 5.6 V. The good performances of device indicated that carbazole oligomers could be the promising candidate for hole-transporting materials, which was attributed to its electron-rich nature of carbazole and its relatively high-energy levels.

Second, in order to investigate the influence of pyrene modification on ethynylene-linked oligocarbazole, type 2 (ITO/PEDOT:PSS(30 nm)/**PyCz5Py** or **Cz3PyCz3**(50 nm)/TPBI(20 nm)/Al (100 nm)) was fabricated, in which 1,3,5-tris(*N*-phenylbenzimidazol-2-yl)benzene (TPBI) was adopted as an electron-transporting and hole-blocking layer and the oligomer with similar molecular length, **PyCz5Py** or **Cz3PyCz3**, was used as emitting as well as hole-transporting layer. Figure 7b shows the EL spectra of both devices. Pyrene-end-capped oligomer, **PyCz5Py**, showed blue EL emission with a peak at 468 nm, while pyrene-centered oligomer, **Cz3PyCz3**, exhibited green emission with a peak at 516 nm. Such a color tuning was consistent with those of PL emission in solutions and in solid states due to the different positions of pyrene at oligomer backbone. Moreover, EL spectra of pyrene-modified carbazoles were quite similar to their PL spectra in thin neat films, which indicated that both PL and EL emissions originated from the same radiative-decay process of singlet excitons.[27] Furthermore, devices based on **Cz3PyCz3** exhibited better performances than those of device based on **PyCz5Py**, such as a maximum brightness of 1782 cd/m^2 at 13.5 V, a high maximum external quantum efficiency of 0.69%, luminence efficiency of 1.87 cd/A, and so on. This was attributed to the lower LUMO energy level of **Cz3PyCz3** (−2.70 eV) than that of **PyCz5Py**, which was beneficial for electron transfer from TPBI layer to emitting layer. Charge recombination mainly took place and was confined in the low-band gap segment pyrene, while attached carbazoles mainly transport holes only because of short conjugation length.

Finally, the bifunctional property (light-emitting property and hole-transport ability) of **PyCz4** was revealed. Four types of devices with different architecture were comparatively fabricated. They were type 1 (ITO/PEDOT:PSS(30 nm)/**PyCz4**(50 nm)/Al(100 nm)), type 2 (ITO/PEDOT:PSS(30 nm)/**PyCz4**(50 nm)/TPBI(20 nm)/Al(100 nm), type 3 (ITO/PEDOT:PSS(30 nm)/**PyCz4**(50 nm)/Alq3(45 nm)/Al(100 nm), and type 4 (ITO/PEDOT:PSS(30 nm)/**PyCz4**(50 nm)/BCP(15 nm)/Alq3(45 nm)/Al(100 nm). Their energy levels are displayed in Figure 8. 2,9-Dimethyl-4,7-diphenyl-1,10-phenanthroline (BCP) was used as a hole-blocking layer. Figure 7c shows the EL spectra of **PyCz4** in four devices. The single-layer device (type 1) exhibited an emission peak at 468 nm. The performance of this device was rather poor because of the unbalance of holes and electrons. There was a quite small barrier of 0.08 eV for holes transporting from ITO/PEDOT:PSS to **PyCz4**, which facilitated hole transport, while there was a large barrier of 1.81 eV between **PyCz4** and Al which almost forbid electron transport from Al to **PyCz4**. The double-layer device (type 2) exhibited identical emission spectra but improved performances with respect to those of the type 1 device, which should be attributed to the introduction of electron-transporting as well as hole-blocking layer (TPBI). The identical blue emission (468 nm) coming from **PyCz4** in both type 1 and type 2 devices suggested that **PyCz4** could serve as a blue-light emitter in OLEDs. The type 3 device showed a red-shifted EL emission with a peak at 524 nm coming from Alq3, and no emission from **PyCz4** was observed. It indicated that **PyCz4** functioned as hole-transporting material here, and charge recombination took place at the Alq3 layer. Interestingly, the type 4 device with an additional hole-blocking layer (BCP) between **PyCz4** and Alq3 presented the emission at 504 nm. This emission should be the combination of the emissions from **PyCz4** and Alq3. Furthermore, devices with an electron-transporting layer exhibited better performances than those without it, such as low turn-on voltages (3.4−4.1 V), high external efficiency (0.40−0.65%), and maximum brightness (987 cd/m^2 at 10 V−1891 cd/m^2 at 8.5 V). Table 2 summarizes the performances of all devices.

3. Conclusions

In conclusion, a series of pyrene-modified, ethynylene-linked oligocarbazoles were synthesized by a stepwise route involving a Sonogashira coupling reaction. Ethynylene linkages at the 3- and 6-positions of carbazoles resulted in a zigzag shape of molecular backbones. This kind of structure defined conjugation length of molecules and suppressed red shifts in absorption and emission spectra of oligomers in solutions when oligomer's size elongated through carbazole accumulation. Furthermore, introduction of pyrene unit(s) into different positions of oligomers tuned molecules' emission wavelength effectively. Meanwhile, the fluorescence quantum efficiency was improved significantly. OLEDs with different architectures based on these oligomers were fabricated and investigated. The results indicated that **Cz5** and **Cz7** without pyrene could be used as hole-transporting materials only, while pyrene-modified oligomers were of both

(27) Shih, P.-I.; Tseng, Y.-H.; Wu, F.-I.; Dixit, A. K.; Shu, C.-F. *Adv. Funct. Mater.* **2006**, *16*, 1582.

light-emitting properties and hole-transport abilities. Incorporation of low-band gap fluorophore into homopolymer should be a good way to generate bifuncitonal or multifunctional optoelectronic materials.

Experimental Section

Compounds **3, 4** and **6** were prepared following a method similar to that of ref 28.

3-Ethynyl-9-heptyl-9*H*-carbazole (3): ^{1}H NMR ($CDCl_3$) δ 0.86 (t, 3 H, J = 7.0 Hz), 1.23−1.27 (m, 4 H), 1.30−1.38 (m, 4 H), 1.83−1.88 (m, 2 H), 3.06 (s, 1 H), 4.28 (t, 2 H, J = 7.5 Hz), 7.23−7.26 (m, 1 H), 7.33 (d, 1 H, J = 8.5 Hz), 7.40 (d, 1 H, J = 8.5 Hz), 7.46−7.49 (m, 1 H), 7.59 (dd, 1 H, J_1 = 8.5 Hz, J_2 = 1.5 Hz), 8.07 (d, 1 H, J = 8.0 Hz), 8.25 (s, 1 H); ^{13}C NMR ($CDCl_3$) δ 14.2, 22.7, 27.4, 29.1, 31.9, 43.4, 75.2, 85.3, 108.8, 109.1, 112.0, 119.5, 120. 7, 122.5, 122.9, 124.8, 126.3, 129.8, 140.5, 141.0; MS (EI) (*m/z*) 289 (M^+).

9-Heptyl-3,6-diiodo-9*H*-carbazole (4): ^{1}H NMR ($CDCl_3$) δ 0.85 (t, 3 H, J = 7.0 Hz), 1.22−1.31 (m, 8 H), 1.79−1.82 (m, 2 H), 4.20 (t, 2 H, J = 7.0 Hz), 7.16 (d, 2 H, J = 9.0 Hz), 7.70 (dd, 2 H, J_1 = 8.5 Hz, J_2 = 1.5 Hz), 8.32 (d, 2 H, J = 1.0 Hz); ^{13}C NMR ($CDCl_3$) δ 14.3, 22.8, 27.4, 29.1, 29.2, 31.9, 43.5, 81.9, 111.1, 124.2, 129.5, 134.7, 139.7; MS (ESI) (*m/z*) 517.8 (M^+).

3,6-Diethynyl-9-heptyl-9*H*-carbazole (6): ^{1}H NMR ($CDCl_3$) δ 0.85 (t, 3 H, J = 7.5 Hz), 1.21−1.26 (m, 4 H), 1.31−1.34 (m, 4 H), 1.80−1.86 (m, 2 H), 3.07 (s, 2 H), 4.25 (t, 2 H, J = 7.5 Hz), 7.32 (d, 2 H, J = 8.5 Hz), 7.60 (dd, 2 H, J_1 = 8.0 Hz, J_2 = 2.0 Hz), 8.21 (d, 2 H, J = 1.5 Hz); ^{13}C NMR ($CDCl_3$) δ 14.3, 22.8, 27.4, 29.2, 31.9, 43. 6, 75.7, 85.0, 109.2, 112.9, 122.5, 125.0, 130.4, 140.9; MS (EI) (*m/z*) 313 (M^+).

General Procedure for the Synthesis of Compounds 7, 10, 11, 14, PyCz3, PyCz4, PyCz3Py, PyCz5Py, Cz3PyCz3, Cz5, and Cz7. These compounds were obtained following an essentially similar procedure. An illustrative example is provided for **7**.

9-Heptyl-3-((9-heptyl-9*H*-carbazol-3-yl)ethynyl)-6-iodo-9*H*-carbazole (7). Compound **3** (289 mg, 1 mmol), compound **4** (1551 mg, 3 mmol), cuprous iodide (10 mg, 0.05 mmol), dichlorobis-(triphenylphosphine)palladium(II) (3.5 mg, 0.005 mmol), triphenylphosphine (5 mg, 0.02 mmol), and dry triethylamine (100 mL) were placed in a 150 mL round bottle flask equipped with a Teflon-covered magnetic stir bar. After the solution was purged with nitrogen for 30 min, it was refluxed under nitrogen for 4 h. The reaction mixture was filtered, and the filtrate was evaporated under reduced pressure. The residue was purified through column chromatography (silica gel, hexane/methylene chloride as eluent). In this way, 448 mg (72% yield) of **7** was obtained: ^{1}H NMR ($CDCl_3$) δ 0.85−0.88 (m, 6H), 1.25−1.29 (m, 8H), 1.33−1.39 (m, 8H), 1.84−1.90 (m, 4H), 4.26 (t, 2H, J = 7.0 Hz), 4.30 (t, 2H, J = 7.0 Hz), 7.19 (d, 1H, J = 8.5 Hz), 7.25−7.28 (m, 1H), 7.36−7.42 (m, 3H), 7.47−7.51 (m, 1H), 7.67−7.73 (m, 3H), 8.11 (d, 1H, J = 7.5 Hz), 8.26 (s, 1H), 8.33 (s, 1H), 8.40 (d, 1H, J = 1.5 Hz); ^{13}C NMR ($CDCl_3$) δ 14.3, 22.8, 27.5, 29.2, 29.3, 31.9, 32.0, 43.5, 43.6, 81.9, 88.6, 89.4, 109.0, 109.2, 111.2, 113.9, 114.8, 119.5, 120.8, 121.8, 122.8, 123.1, 124.1, 125.3, 126.3, 129.4, 129.6, 130.1, 134.4, 140.0, 140.2, 141.1; MS (MALDI-TOF) (*m/z*) 678.6 (M^+).

9-Heptyl-3-((9-heptyl-6-((9-heptyl-9*H*-carbazol-3-yl)ethynyl)-9*H*-carbazol-3-yl)ethynyl)-6-iodo-9*H*-carbazole (10): 67% yield; ^{1}H NMR ($CDCl_3$) δ 0.84−0.89 (m, 9H), 1.25−1.28 (m, 12H), 1.32−1.40 (m, 12H), 1.82−1.89 (m, 6H), 4.23 (t, 2H, J = 7.5 Hz), 4.27−4.30 (m, 4H), 7.17 (d, 1H, J = 8.5 Hz), 7.26−7.27 (m, 1H), 7.34−7.41 (m, 5H), 7.47−7.50 (m, 1H), 7.68−7.71 (m, 5H), 8.12 (d, 1H, J = 7.5 Hz), 8.26 (s, 1H), 8.33 (s, 2H), 8.35 (s, 1H), 8.40 (d, 1H, J = 0.5 Hz); ^{13}C NMR ($CDCl_3$) δ 14.3, 22.8, 27.5, 29.2, 29.3, 31.9, 32.0, 43.4, 43.5, 43.6, 81.9, 88.9, 89.0, 89.3, 109.0, 109.1, 109.2, 111.2, 114.0, 114.5, 114.7, 119.5, 120.8, 121.8, 122.8, 123.1, 124.1, 124.2, 125.2, 126.2, 129.5, 129.6, 129.8, 130.1, 134.4, 140.0, 140.2, 140.4, 140.5, 141.0; MS (MALDI-TOF) (*m/z*) 965.8 (M^+).

9-Heptyl-3-iodo-6-(pyren-1-ylethynyl)-9*H*-carbazole (11): 70% yield; ^{1}H NMR ($CDCl_3$) δ 0.86 (t, 3H, J = 7.0 Hz), 1.21−1.31 (m, 8H), 1.80−1.82 (m, 2H), 4.19 (t, 2H, J = 7.0 Hz), 7.14 (d, 1H, J = 8.5 Hz), 7.36 (d, 1H, J = 8.0 Hz), 7.70 (dd, 1H, J_1 = 8.5 Hz, J_2 = 1.5 Hz), 7.80 (dd, 1H, J_1 = 8.5 Hz, J_2 = 1.5 Hz), 7.99−8.06 (m, 3H), 8.11 (d, 1H, J = 8.0 Hz), 8.16−8.22 (m, 4H), 8.35 (s, 1H), 8.41 (s, 1H), 8.72 (d, 1H, J = 8.5 Hz); ^{13}C NMR ($CDCl_3$) δ 14.3, 22.8, 27.4, 29.1, 29.3, 31.9, 43.5, 82.2, 87.5, 96.7, 109.2, 111.2, 114.3, 118.7, 121.9, 124.4, 124.6, 124.8, 125.2, 125.6, 125.7, 126.0, 126.4, 127.5, 128.1, 128.4, 129.6, 129.7, 130.2, 131.1, 131.4, 131.5, 131.9, 134.5, 140.1, 140.3; MS (MALDI-TOF) (*m/z*) 615.2 (M^+).

9-Heptyl-3-((9-heptyl-6-(pyren-1-ylethynyl)-9*H*-carbazol-3-yl-)ethynyl)-6-iodo-9*H*-carbazole (14): 62% yield; ^{1}H NMR ($CDCl_3$) δ 0.85−0.89 (m, 6H), 1.24−1.37 (m, 16H), 1.82−1.85 (m, 2H), 1.88−1.90 (m, 2H), 4.23 (t, 2H, J = 7.5 Hz), 4.30 (t, 2H, J = 7.5 Hz), 7.17 (d, 1H, J = 9.0 Hz), 7.35−7.44 (m, 3H), 7.69−7.72 (m, 3H), 7.84 (dd, 1H, J_1 = 8.5 Hz, J_2 = 1.5 Hz), 8.01−8.09 (m, 3H), 8.15 (d, 1H, J = 7.5 Hz), 8.19−8.27 (m, 5H), 8.38 (d, 1H, J = 1.0 Hz), 8.40 (d, 1H, J = 1.5 Hz), 8.46 (d, 1H, J = 1.5 Hz), 8.77 (d, 1H, J = 7.5 Hz); ^{13}C NMR ($CDCl_3$) δ 14.3, 22.8, 27.5, 29.2, 29.3, 31.9, 32.0, 43.5, 43.6, 81.9, 87.4, 89.1, 89.2, 96.9, 109.2, 109.3, 111.2, 114.3, 114.7, 118.8, 121.8, 122.8, 122.9, 124.2, 124.3, 124.5, 124.7, 124.8, 125.2, 125.7, 125.7, 126.0, 126.4, 127.6, 128.2, 128.4, 129.6, 129.7, 129.9, 130.0, 130.1, 131.2, 131.4, 131.6, 132.0, 134.4, 140.0, 140.2, 140.5, 140.8; MS (MALDI-TOF) (*m/z*) 902.5 (M^+).

9-Heptyl-3-((9-heptyl-6-((9-heptyl-9*H*-carbazol-3-yl)ethynyl)-9*H*-carbazol-3-yl)ethynyl)-6-(pyren-1-ylethynyl)-9*H*-carbazole (PyCz3): 55% yield; ^{1}H NMR ($CDCl_3$) δ 0.84−0.89 (m, 9H), 1.25−1.27 (m, 12H), 1.35−1.36 (m, 12H), 1.85−1.91 (m, 6H), 4.26−4.31 (m, 6H), 7.22−7.25 (m, 1H), 7.36−7.49 (m, 7H), 7.68−7.74 (m, 4H), 7.83 (dd, 1H, J_1 = 8.5 Hz, J_2 = 1.0 Hz), 7.99−8.26 (m, 9H), 8.34−8.35 (m, 3H), 8.40 (s, 1H), 8.47 (s, 1H), 8.77 (d, 1H, J = 9.5 Hz); ^{13}C NMR ($CDCl_3$) δ 14.3, 22.8, 27.5, 29.2, 29.3, 32.0, 43.5, 43.6, 87.4, 88.9, 89.1, 89.3, 96.9, 109.0, 109.1, 109.2, 109.3, 114.0, 114.3, 114.6, 114.7, 114.9, 118.8, 119.5, 120. 8, 122.8, 122.9, 123.0, 123.1, 124.1, 124.2, 124.3, 124.5, 124.7, 124.8, 125.6, 125.7, 126.1, 126.6, 126.4, 127.6, 128.1, 128.4, 129.5, 129.7, 129.9, 130.0, 131.2, 131.5, 131.6, 132.0, 140.2, 140.5, 140.8, 141.0; MS (MALDI-TOF) (*m/z*) 1063.9 (M^+). Anal. Calcd for $C_{79}H_{73}N_3$: C, 89.14; H, 6.91; N, 3.95. Found: C, 89.11; H, 6.98; N, 3.92.

9-Heptyl-3-((9-heptyl-6-((9-heptyl-6-((9-heptyl-9*H*-carbazol-3-yl)ethynyl)-9*H*-carbazol-3-yl)ethynyl)-9*H*-carbazol-3-yl)ethynyl)-6-(pyren-1-ylethynyl)-9*H*-carbazole (PyCz4): 46% yield; ^{1}H NMR ($CDCl_3$) δ 0.83−0.88 (m, 12H), 1.24−1.30 (m, 16H), 1.35 (m, 16H), 1.80−1.88 (m, 8H), 4.21 (t, 2H, J = 7.5 Hz), 4.25−4.29 (m, 6H), 7.21−7.24 (m, 1H), 7.31−7.46 (m, 9H), 7.65−7.74 (m, 6H), 7.82 (dd, 1H, J_1 = 8.5 Hz, J_2 = 2.0 Hz), 7.97−8.24 (m, 10H), 8.32−8.35 (m, 4H), 8.40 (s, 1H), 8.46 (s, 1H), 8.76 (d, 1H, J = 9.0 Hz); MS (MALDI) (*m/z*) 14.3, 22.8, 27.5, 29.2, 29.3, 31.9, 32.0, 43.4, 43.6, 87.4, 88.9, 89.1, 89.2, 89.3, 89.4, 96.9, 108.9, 109.1, 109.2, 109.3, 114.0, 114.3, 114.6, 114.7, 114.9, 118.8, 119.4, 120.8, 122.8, 123.0, 123.1, 124.1, 124.2, 124.3, 124.5, 124.7, 124.8, 125.6, 125.7, 126.0, 126.2, 126.4, 127.5, 128.1, 128.4, 129.4, 129.7, 129.8, 129.9, 130.0, 131.1, 131.4, 131.6, 132.0, 140.1, 140.4, 140.5, 140. 8, 141.0; MS (MALDI-TOF) (*m/z*) 1351.0 (M^+). Anal. Calcd for $C_{100}H_{94}N_4$: C, 88.85; H, 7.01; N, 4.14. Found: C, 88.90; H, 7.07; N, 4.21.

6,6′-(9-Heptyl-9*H*-carbazole-3,6-diyl)bis(ethyne-2,1-diyl)bis-(9-heptyl-3-(pyren-1-ylethynyl)-9*H*-carbazole) (PyCz3Py): 58% yield; ^{1}H NMR ($CDCl_3$) δ 0.85−0.88 (m, 9H), 1.25−1.28 (m, 12H), 1.33−1.37 (m, 12H), 1.86−1.88 (m, 6H), 4.23−4.27 (m, 6H), 7.35−7.40 (m, 6H), 7.70−7.74 (m, 4H), 7.81 (dd, 2H, J_1 = 8.5 Hz, J_2 = 1.0 Hz), 7.93−8.01 (m, 6H), 8.06 (d, 2H, J = 8.0 Hz), 8.12 (d, 2H, J = 7.5 Hz), 8.16−8.20 (m, 6H), 8.35 (s, 2H), 8.39

(28) (a) Beginn, C.; Grazulevicius, J. V.; Strohriegl, P. *Macromol. Chem. Phys.* **1994**, *195*, 2353. (b) Grigalevicius, S.; Grazulevicius, J. V.; Gaidelis, V.; Jankauskas, V. *Polymer* **2002**, *43*, 2603.

(s, 2H), 8.45 (s, 2H), 8.72 (d, 2H, $J = 9.5$ Hz); ^{13}C NMR ($CDCl_3$) δ 14.1, 22.6, 27.3, 29.0, 29.1, 31.8, 43.4, 87.2, 89.0, 89.1, 96.7, 109.0, 109.1, 114.1, 114.4, 114.6, 118.6, 122.6, 122.7, 124.0, 124.1, 124.3, 124.4, 124.6, 125.4, 125.5, 125.8, 126.1, 127.3, 127.8, 128.1, 129.4, 129.6, 129.7, 130.9, 131.2, 131.3, 131.7, 140.3, 140.5; MS (MALDI-TOF) (*m/z*) 1287.6 (M^+). Anal. Calcd for $C_{97}H_{81}N_3$: C, 90.40; H, 6.34; N, 3.26. Found: C, 90.42; H, 6.31; N, 3.22.

6,6′-(9-Heptyl-9*H*-carbazole-3,6-diyl)bis(ethyne-2,1-diyl)bis-(9-heptyl-3-((9-heptyl-6-(pyren-1-ylethynyl)-9*H*-carbazol-3-yl)-ethynyl)-9*H*-carbazole) (PyCz5Py): 45% yield; ^{1}H NMR ($CDCl_3$) δ 0.84−0.88 (m, 15H), 1.22−1.25 (m, 20H), 1.28−1.32 (m, 20H), 1.79−1.90 (m, 10H), 4.13 (t, 4H, $J = 7.5$ Hz), 4.19 (t, 4H, $J = 7.5$ Hz), 4.28 (t, 2H, $J = 7.0$ Hz), 7.26−7.30 (m, 6H), 7.35−7.39 (m, 4H), 7.65−7.23 (m, 8H), 7.80 (dd, 2H, $J_1 = 8.5$ Hz, $J_2 = 1.5$ Hz), 7.96−7.98 (m, 4H), 8.02 (d, 2H, $J = 9.0$ Hz), 8.07 (d, 2H, $J = 8.0$ Hz), 8.14 (d, 2H, $J = 7.5$ Hz), 8.18−8.22 (m, 6H), 8.31 (m, 6H), 8.38 (s, 2H), 8.40 (s, 2H), 8.74 (d, 2H, $J = 8.0$ Hz); ^{13}C NMR ($CDCl_3$) δ 14.3, 22.8, 27.4, 27.5, 29.2, 29.3, 32.0, 43.4, 43.5, 87.4, 89.2, 89.3, 97.0, 109.1, 109.2, 114.2, 114.6, 114.7, 114.8, 118.8, 122.7, 122.8, 122.9, 124.1, 124.2, 124.5, 124.6, 124.8, 125.5, 125.7, 126.0, 126.3, 127.5, 128.0, 128.3, 129.6, 129.7, 129.8, 129.9, 131.0, 131.4, 131.5, 131.9, 140.3, 140.4, 140.7; MS (MALDI-TOF) (*m/z*) 1863.1 (M^+). Anal. Calcd for $C_{139}H_{123}N_5$: C, 89.59; H, 6.65; N, 3.76. Found: C, 89.60; H, 6.61; N, 3.77.

1,8-Bis((9-heptyl-6-((9-heptyl-6-((9-heptyl-9*H*-carbazol-3-yl)-ethynyl)-9*H*-carbazol-3-yl)ethynyl)-9*H*-carbazol-3-yl)ethynyl)-pyrene (Cz3PyCz3): 39% yield; ^{1}H NMR ($CDCl_3$) δ 0.82−0.88 (m, 18H), 1.21−1.35(m, 48H), 1.78−1.88 (m, 12H), 4.14 (t, 4H, $J = 7.0$ Hz), 4.21−4.27 (m, 8H), 7.21−7.24 (m, 2H), 7.25−7.30 (m, 4H), 7.31−7.40 (m, 10H), 7.64−7.68 (m, 8H), 7.85 (dd, 2H, $J_1 = 8.5$ Hz, $J_2 = 1.0$ Hz), 8.02 (s, 2H), 8.08−8.12 (m, 4H), 8.24−8.29 (m, 8H), 8.34 (d, 2H, $J = 1.0$ Hz), 8.44 (d, 2H, $J = 1.5$ Hz), 8.9 (s, 2H); ^{13}C NMR ($CDCl_3$) δ 14.3, 22.8, 27.5, 29.2, 29.3, 29.8, 31.3, 31.5, 31.9, 43.4, 43.5, 87.5, 88.9, 89.2, 89.3, 89.4, 97.5, 108.9, 109.1, 109.3, 114.0, 114.2, 114.6, 114.7, 114.8, 117.4, 119.4, 119.5, 120.8, 122.8, 122.9, 123.1, 124.0, 124.1, 124.2, 124.5, 124.6, 125.0, 125.2, 125.8, 126.2, 126.7, 126.8, 127.0, 127.1, 127.9, 128.2, 129.4, 129.5, 129.7, 129.8, 129.9, 130.0, 131.3, 132.0, 140.1, 140.4, 140.8, 141.0. MS (MALDI-TOF) (*m/z*) 1925.4 (M^+). Anal. Calcd for $C_{142}H_{136}N_6$: C, 88.52; H, 7.11; N, 4.36. Found: C, 88.60; H, 7.05; N, 4.43.

6,6′-(9-Heptyl-9*H*-carbazole-3,6-diyl)bis(ethyne-2,1-diyl)bis-(9-heptyl-3-((9-heptyl-9*H*-carbazol-3-yl)ethynyl)-9H-carbazole) (Cz5): 61% yield; ^{1}H NMR ($CDCl_3$) δ 0.84−0.88 (m, 15H), 1.24−1.28 (m, 20H), 1.34−1.36 (m, 20H), 1.83−1.89 (m, 10H), 4.23−4.29 (m, 10H), 7.22−7.25 (m, 2H), 7.34−7.39 (m, 10H), 7.45−7.48 (m, 2H), 7.67−7.72 (m, 8H), 8.10 (d, 2H, $J = 7.5$ Hz), 8.34−8.35 (m, 8H); ^{13}C NMR ($CDCl_3$) δ 14.3, 22.8, 27.5, 29.2, 29.3, 32.0, 43.4, 43.6, 88.9, 89.1, 89.3, 108.9, 109.1, 109.2, 114.0, 114.6, 114.7, 119.4, 120.8, 122.7, 122.8, 123.1, 124.0, 124.2, 129.4, 129.8, 129.9, 140.1, 140.4, 140.5, 141.0; MS (MALDI-TOF) (*m/z*) 1414.0 (M^+). Anal. Calcd for $C_{103}H_{107}N_5$: C, 87.43; H, 7.62; N, 4.95. Found: C, 87.47; H, 7.65; N, 4.90.

6,6′-(9-Heptyl-9*H*-carbazole-3,6-diyl)bis(ethyne-2,1-diyl)bis-(9-heptyl-3-((9-heptyl-6-((9-heptyl-9*H*-carbazol-3-yl)ethynyl)-9*H*-carbazol-3-yl)ethynyl)-9*H*-carbazole) (Cz7): 51% yield; ^{1}H NMR ($CDCl_3$) δ 0.86−0.90 (m, 21 H), 1.27 (m, 28H), 1.36 (m, 28H), 1.85−1.91 (m, 14H), 4.24−4.28 (m, 12H), 4.31−4.34 (m, 2H), 7.24−7.27 (m, 2H), 7.35−7.42 (m, 14H), 7.47−7.50 (m, 2H), 7.69−7.75 (m, 12H), 8.12 (d, 2H, $J = 8.0$ Hz), 8.34−8.39 (m, 12H); ^{13}C NMR ($CDCl_3$) δ 14.3, 22.8, 27.5, 29.2, 29.3, 32.0, 43.4, 43.5, 88.9, 89.2, 89.3, 108.9, 109.1, 109.2, 114.0, 114.6, 114.7, 119.4, 120.8, 122.8, 122.9, 123.1, 124.0, 124.2, 126.2, 129.7, 129.8, 129.9, 140.1, 140.4, 140.5, 141.0; MS (MALDI-TOF) (*m/z*) 1988.4 (M^+). Anal. Calcd for $C_{145}H_{149}N_7$: C, 87.52; H, 7.55; N, 4.93. Found: C, 87.47; H, 7.59; N, 4.99.

General Procedure for the Synthesis of the Compounds (9 and 13). Both compounds were obtained following an essentially similar procedure. An illustrative example is provided for **9**.

3-Ethynyl-9-heptyl-6-((9-heptyl-9*H*-carbazol-3-yl)ethynyl)-9*H*-carbazole (9). Compound **7** (678 mg, 1 mmol), 3-methyl-1-butyn-3-ol (126 mg, 1.5 mmol), cuprous iodide (10 mg, 0.05 mmol), dichlorobis(triphenylphosphine)palladium(II) (3.5 mg, 0.005 mmol), triphenylphosphine (5 mg, 0.02 mmol), and dry triethylamine (100 mL) were placed in a 150 mL round bottle flask equipped with a Teflon-covered magnetic stir bar. After the solution was purged with nitrogen for 30 min, it was refluxed under nitrogen for 8 h. The reaction mixture was filtered, and the filtrate was evaporated under reduced pressure. The residue was purified by column chromatography (silica gel, hexane/methylene chloride as eluent) to get **8**. Then **8**, 500 mg of KOH, and 100 mL of 2-propanol were placed in a 150 mL round-bottom flask equipped with a Teflon-covered magnetic stir bar. After the solution was purged with nitrogen for 30 min, it was refluxed under nitrogen for 4 h. The solvent was then removed, and the crude product was purified by column chromatography (silica gel, hexane/methylene chloride as eluent) to afford **9** (576 mg, 75% total yield): ^{1}H NMR ($CDCl_3$) δ 0.85−0.88 (m, 6H), 1.23−1.28 (m, 8H), 1.33−1.38 (m, 8H), 1.84−1.89 (m, 4H), 3.08 (s, 1H), 4.25−4.30 (m, 4H), 7.24−7.27 (m, 1H), 7.32 (d, 1H, $J = 8.5$ Hz), 7.35−7.41 (m, 3H), 7.46−7.50 (m, 1H), 7.60 (dd, 1H, $J_1 = 8.5$ Hz, $J_2 = 1.0$ Hz), 7.67−7.70 (m, 2H), 8.11 (d, 1H, $J = 7.5$ Hz), 8.25 (d, 1H, $J = 1.5$ Hz), 8.29 (d, 1H, $J = 1.5$ Hz), 8.33 (d, 1H, $J = 2.0$ Hz); ^{13}C NMR ($CDCl_3$) δ 14.3, 22.8, 27.5, 29.2, 29.3, 31.9, 32.0, 43.5, 43.6, 75.6, 85.2, 88.7, 89.4, 109.0, 109.1, 109.2, 112.7, 114.0, 114.9, 119.5, 120.8, 122.7, 122.8, 123.1, 124.1, 125.1, 126.3, 129.5, 130.0, 130.2, 140.2, 140.5, 140.9, 141.1; MS (MALDI-TOF) (*m/z*) 576.5 (M^+).

3-Ethynyl-9-heptyl-6-(pyren-1-ylethynyl)-9*H*-carbazole (13): 63% total yield; ^{1}H NMR ($CDCl_3$) δ 0.86 (t, 3H, $J = 7.0$ Hz), 1.23−1.28 (m, 4H), 1.31−1.37 (m, 4H), 1.83−1.89 (m, 2H), 3.10 (s, 1H), 4.27 (t, 2H, $J = 7.5$ Hz), 7.34 (d, 1H, $J = 8.5$ Hz), 7.41 (d, 1H, $J = 8.5$ Hz), 7.62 (dd, 1H, $J_1 = 8.5$ Hz, $J_2 = 1.5$ Hz), 7.82 (dd, 1H, $J_1 = 8.5$ Hz, $J_2 = 1.5$ Hz), 8.00−8.09 (m, 3H), 8.13 (d, 1H, $J = 8.0$ Hz), 8.18−8.24 (m, 4H), 8.30 (d, 1H, $J = 1.0$ Hz), 8.42 (d, 1H, $J = 1.5$ Hz), 8.75 (d, 1H, $J = 9.0$ Hz); ^{13}C NMR ($CDCl_3$) δ 14.3, 22.8, 27.5, 29.2, 29.3, 31.9, 43.6, 75.7, 85.1, 87.4, 96.7, 109.2, 109.4, 113.0, 114.5, 118.7, 122.7, 122.8, 124.5, 124.7, 124.8, 125.1, 125.7, 125.8, 126.0, 126.4, 127.6, 128.2, 128.4, 129.7, 130.1, 130.4, 131.2, 131.4, 131.6, 132.0, 140.8, 140.9; MS (MALDI-TOF) (*m/z*) 513.4 (M^+).

Acknowledgment. P.L. thanks the National Natural Science Foundation of China (20374045, 20674070) and the Natural Science Foundation of Zhejiang Province (R404109) for support. We thank Prof. Chuande Wu for his assistance in drawing the molecular models depicted in Figure 4. This work was partially supported by the Major State Basic Research Development Program and the Chinese Academy of Sciences.

Supporting Information Available: General information, OLED fabrication and measurement, NMR and mass spectra of new compounds, and *J-V-L* characteristics and efficiency spectra of OLEDs. This material is available free of charge via the Internet at http://pubs.acs.org.

JO702075R